

Design and Construction of a High-Duty Factor Photocathode Electron Gun*

I.S. Lehrman, I.A. Birnbaum, M. Cole, R.L. Heuer, E. Sheedy
Grumman Aerospace Corporation, 4 Independence Way, Princeton, NJ 08540 USA

I. Ben-Zvi, K. Batchelor, J.C. Gallardo, H.G. Kirk, T. Srinivasan-Rao
Brookhaven National Laboratory, Upton, NY 11973 USA

Abstract

Under a joint collaboration between Grumman and BNL, a high-duty factor ($> 1\%$) photocathode electron gun is being constructed for use at the ATF facility at BNL. This gun was designed as the electron source for the proposed UV FEL Users' Facility at BNL. The thermally induced stresses exceed the yield strength of OFHC copper. For this reason, the gun is fabricated from GlidCop, an aluminum oxide dispersion strengthened copper alloy.

I. INTRODUCTION

The proposed UV FEL User's Facility at BNL[1] will require a photocathode electron gun capable of producing short (< 6 psec) bunches of electrons at high repetition rates (5 kHz), low energy spread ($< 1.0\%$), peak currents in excess of > 300 A (after compression) and a total bunch charge in excess of 3 nC. The emittance of the electron bunches is required to be below 7π mm-mrad (normalized RMS).

The construction of such a gun (Gun II) is nearing completion under a joint Grumman-Brookhaven National Laboratory research collaboration [2]. The starting point for our design is the present 1-1/2 cell BNL photocathode RF gun (Gun I) shown in Fig. 1. Figure 2 shows the layout of Gun II. Gun II consists of 3-1/2 cells which allows beam energies in excess of 9 MeV to be achieved. The beam dynamics of the gun were modeled with the MAGIC[3] particle-in-cell code. This code is used to study the emittance growth of the electron bunches as they are accelerated through the gun, as well as to determine how the operational parameters effect its characteristics (i.e. divergence, momentum spread, energy, current).

The thermal and mechanical properties of the gun were modeled with the ANSYS[4] finite element code. Power deposition profiles were calculated with SUPERFISH[5]. A thermal/structural analysis was performed to determine the temperature profiles and the pressure and thermally induced stresses.

II. BEAM DYNAMICS MODELING

The MAGIC code includes the effects of image currents, space charge and wakefields. The axisymmetric gun geometry (2-D) was modeled with exact gun fields. This is

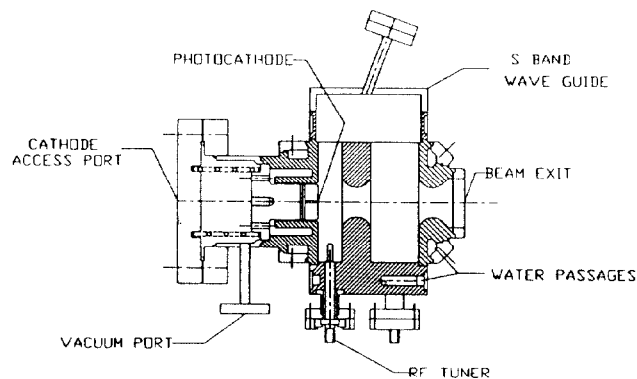


Figure 1. Present BNL 1-1/2 cell gun (Gun I).

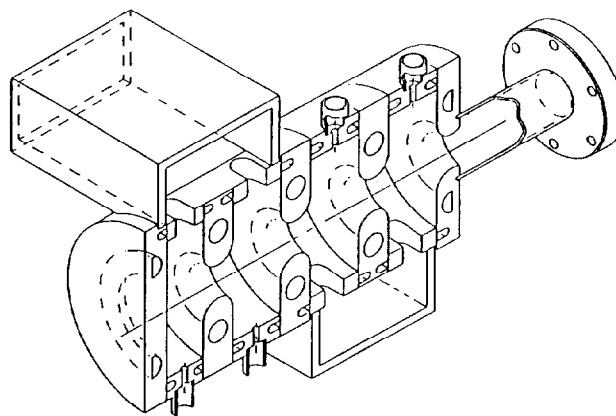


Figure 2. Cutaway view of Gun II showing the locations of the water cooling channels.

accomplished by prescribing the magnetic field for the fundamental TM_{01} cylindrical cavity mode and allowing the cavity to ring while numerically damping out higher order modes. The fields are then stored and used for later runs with particles. Figure 3 shows a vector plot of the electric fields for Gun II.

The advantage of using the MAGIC code is that the field components at the cavity apertures and beam exit are continuous and the method of calculating the space charge forces is inherently more stable. Typical simulations for a 3-1/2 cell gun consisted of a grid 2000×90 (Z x R) with 1500

*This work supported by the Grumman Corporation and the Brookhaven National Laboratory under US DOE contract.

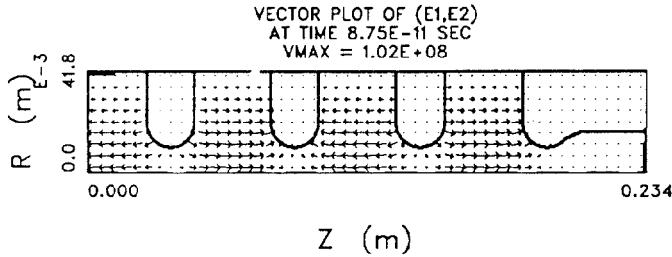


Figure 3. Vector plot from MAGIC of the electric field in the 3-1/2 cell gun (Gun II)

particles. Particles are emitted in nearly any functional form in radius and time to model the laser illumination of the cathode. Table 1 lists the operational parameters for Gun II.

Table 1. Operational parameters of Gun II

Number of cells	1
Laser radius ($1\sigma_r$)	4 mm
Pulse length ($\pm 2\sigma_t$)	8 psec
Cathode electric field (nominal)	100 MV/m
Beam momentum	10 MeV/c
Peak power	12.5 MW
Duty factor	1%
RF frequency	2.856 GHz

Most of our simulations were done for a 1-1/2 cell gun since they require 1/4 of the computer time and uncover most of the underlying physics. The brightness, B , was used as one figure of merit for our gun design. We use the definition:

$$B = \frac{I}{\epsilon_n^2}, \quad I = \frac{Q}{\sqrt{2\pi} \sigma_b}$$

where I is the peak current, ϵ_n is the RMS invariant emittance, Q is the total charge, and σ_b is the bunch length (divided by the speed of light). After the beam exits the gun, it enters a transport line whose function is to match the beam to the linac. In addition, the transport line may serve to magnetically compress the bunch length, resulting in peak currents >1000 amps. The compressibility was determined analytically and used to determine the ideally compressed current.

The divergence of the beam is inversely proportional to γ , the relativistic factor, and the space charge forces are inversely proportional to γ^2 . Simulations of the full 3-1/2 cell gun show that the addition of 2 full cells for the gun (Gun II) will double the momentum of electrons to 10 MeV/c which should result in a bunch that is more easily transported and compressed.

A study was made to determine the effect of varying the length of the half cell on the emittance, divergence and compressibility. It was found that by increasing the length of the half cell from 2.625 cm ($\lambda/4$) to 3.5 cm, the divergence was reduced by 20%, the compressibility increased by a factor of 2, and the effect on the emittance was negligible. The 3.5 cm first cell offers a number of other advantages. The peak

electric field is on the cathode rather than on the aperture as in the previous case. This should allow the cathode field to reach 110 MV/m with the same conditioning that it takes to reach 100 MV/m in the present BNL gun. Table 2 summarizes the beam dynamics modeling for Gun II.

Table 2. Modeling results for Gun II

Charge (nC)	0.5	1.0	3.0
Emittance (π mm-mrad)	2.3	3.4	8.9
Divergence (\times' mrad)	7.9	8.3	9.5
Momentum spread	- 0.2% - 2.0% (selectable)		
Launch phase	55°	59°	63°
Peak current			
Uncompressed (A)	118	220	571
Compressed (A)	2705	4224	7429

III. THERMAL AND MECHANICAL DESIGN

Operation at duty factors of 1% present significant challenges in the heat removal aspects of the gun as well as the pressure and thermally induced stresses and deformations. The half cell of the gun will be 3.5 cm long followed by 3 full cells each 5.25 cm ($\lambda/2$) in length. The longer cell simplifies the construction of the gun by reduced the space constraints. The peak power in the gun is 12.5 MW, thus an average power of 125 kW must be removed from the structure. Since Gun II will utilize a copper cathode, the cathode wall will be constructed of a solid GlidCop plate without penetrations. The cathode plate, four cylindrical spool pieces and four aperture pieces will be brazed together. The cathode plate is a 0.75 cm long cylinder 12.25 cm in diameter, with coolant channels milled in a circular pattern. A second 0.75 cm long cylinder is brazed on the back to enclose the channels. A 2.5 cm long cylindrical spool piece is used to connect the photocathode to the aperture. The spool pieces for the full cells are 3.25 cm long. All of the spool piece are cooled by circular channel machined into each end. Each aperture is designed as two cylindrical pieces, 1.0 cm long with two coolant channels milled in a circular pattern, which are brazed together. The aperture opening is a separate machining operation.

We have chosen to use GlidCop-25, an aluminum oxide dispersion strengthened copper alloy, which combines good thermal, electrical, and structural properties. The GlidCop will be electroplated with OFHC copper to provide the good electrical conductivity for the cavity and a barrier for the silver based braze alloys.

The thermal management of the gun requires heat removal from a cavity only 8.31 cm in diameter with peak power densities of 22 kW/cm². The mode of heat transfer chosen is turbulent forced convection, the Dittus-Boelter heat transfer correlation was used. The heat removal is provided by pumping pressurized water through strategically placed coolant channels.

The power density was supplied by the SUPERFISH code for the cavity configurations evaluated. The power density in the longer half cell is decreased by nearly 15%. The operating

pressure and temperature distributions are input to the structural model and the pressure and thermally induced deformations and stresses are calculated. The resulting displacements are evaluated to determine the variation in cavity deformations impacting the frequency and tuning of the cavity. The stresses are evaluated and compared to the various stress categories in the ASME Boiler and Pressure Vessel Code.

The temperature distribution (3-D) shows that the peak temperature of the gun should reach about 144 °C which corresponds to a frequency shift of 4.4 MHz. The maximum Von Mises stress is less than 21 ksi (145 MPa) with an allowable of 31 ksi (214 MPa). 3-D modeling indicates no significant increases in either the temperatures or stresses occur near the coupling slots. Though these stress levels are well within the allowable levels for GlidCop, they exceed the allowable levels for OFHC copper (Yield Stress = 11 ksi).

IV. RF DYNAMICS

The design of Gun II requires that π -mode phasing be maintained between cells 1 and 2 and between cells 3 and 4. In addition, we would like to vary the phase smoothly between cells 2 and 3. The arrangement of the coupling slots and the distance of the waveguide short from the coupling slots ($\lambda/4$) preferentially couples to the π -mode. Figure 4 shows the mode separation and relative amplitudes for the 0 and π -modes when two adjacent cells are driven with a single loop coupler or with the waveguide. Notice that the single loop excites the 0-mode most strongly by aperture coupling to the second cavity. By comparison, the waveguide most strongly excites the π -mode. The coupling constant is approximately 5×10^{-4} .

In order to match the waveguide to the gun, the coupling slots must be sized for critical coupling. The coupling is dependent on the Q of the cavity, therefore, the coupling slots will be slightly undersized and the gun will be brazed together. The final matching of the waveguide to the gun will then be achieved by shimming the height of the waveguide above the coupling slots. This method is preferred over cutting the coupling slots since the resonant frequency of the cavity is significantly influenced by the size of the coupling slots.

V. GUN STATUS

The GlidCop aperture sections and cathode plates have been brazed into assemblies and have been leak checked. A 1 cm thick disk was brazed between the aperture halves of the aperture which separates cells 2 and 3. This additional thickness was found to sufficiently reduce the coupling between cells 2 and 3. The apertures were then machined to achieve the final dimensions. The apertures and cathode were polished with diamond paper to achieve better than a 4 micro-inch finish. The ring sections have been completed as well. The apertures and rings have been clamped together and final tuning is nearly complete. We have been able to achieve better than 20% field tilt between adjacent cells.

After the rings have been polished, all of the GlidCop pieces will be copper plated with 0.0015" of copper. The

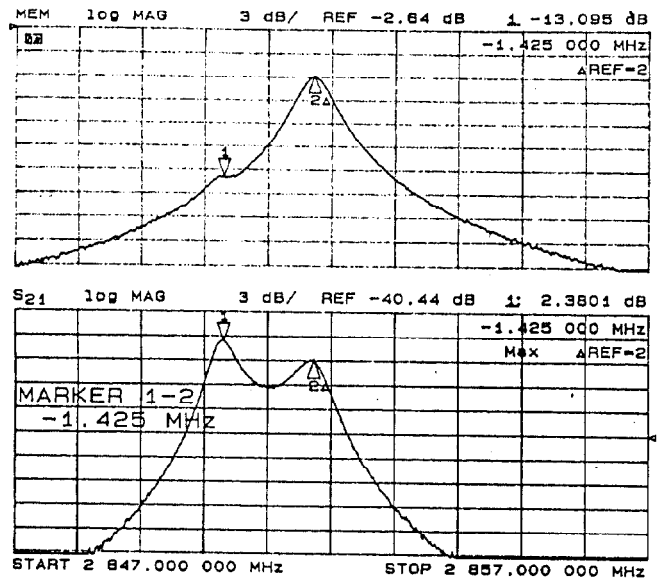


Figure 4. Network analyzer plots of the mode structure in Gun II. Points 1 and 2 indicate the locations of the 0-mode and π -modes, respectively. Waveguide driven (top) and loop driven (bottom).

assemblies will then be remeasured and tuned by polishing with copper wool in order to achieve 5% field tilt between adjacent cells.

Once the rings and apertures are in final form, the stainless cooling tubes (~60 pieces) and exit tube will be brazed to the GlidCop sections. The aperture and ring sections will then be brazed together and final frequency measurements will be made on the gun. If it is necessary to correct for the frequency of the cells at this point, material can be removed from the coupling slots to lower the frequency of the cells. A shim will be fitted and sized in the waveguide to increase the coupling to slightly beyond critical coupling. The final step will be to braze the waveguides to the gun.

VI. REFERENCES

- [1] I. Ben-Zvi, L.F. Di Mauro, S. Krinsky, M.G. White and L.H. Yu, Nucl. Instr. and Meth. A304 (1991) 181.
- [2] I. S. Lehrman, I. A. Birnbaum, M. Cole, *et al*, Proceedings of the 1992 Linear Accelerator Conference, Ottawa, CA, August 24-28, 1992 (1992)280.
- [3] G.D. Warren, L. Ludeking, J. McDonald, K. Nguyen and B. Goplen, Proc. Conf. on Computer Codes and the Linear Accelerator Community, Los Alamos National Laboratory, Jan 22-25, 1990, ed. R. Cooper, LA-11857-Z (1990) 57.
- [4] ANSYS engineering analysis system, Rev 4.3A, Swanson Analysis Systems Inc. Houston, Pa. (1987).
- [5] M.T. Menzel and H.K. Stokes, Users guide for the POISSON/SUPERFISH group of codes, Los Alamos Natl. Lab. Rep. LA-UR-87-15 (Jan. 1987).